Geophys. Astrophys. Fluid Dynamics, Vol. 49, pp. 129–141
Reprints available directly from the publisher
Photocopying permitted by license only

ON THE NONLINEAR STABILITY OF DYNAMO MODELS

A. BRANDENBURG and I. TUOMINEN

Observatory and Astrophysics Laboratory, University of Helsinki, Tähtitorninmäki, SF-00130 Helsinki, Finland

D. MOSS

Department of Mathematics, The University, Manchester M13 9PL, England

(*Received 28 September 1988; in final form 13 February 1989*)

The stability of nonlinear mean-field dynamo models in spherical geometry has been investigated numerically. Assuming axisymmetry and incompressibility we find stable stationary solutions of both even and odd parity over a range of four decades in the Taylor number. Furthermore, we extend studies on solutions with "mixed parity", which have been found previously for an $\alpha\omega$-dynamo model, neglecting here, however, the explicit feedback on the mean motions. Plots of trajectories in phase space and Poincaré maps, showing intersections of the trajectories with certain hyperplanes in phase space, reveal that the solution lies on a torus for some of these models.

KEY WORDS: Hydromagnetic dynamos, nonlinear stability.

1. INTRODUCTION

The stability of simple nonlinear $\alpha\omega$-dynamos has been studied by Kleeorin and Ruzmaikin (1984), who found a simple criterion for the stability of the solution at the *first* bifurcation from the trivial solution. Recently Krause and Meinel (1988) found that the solutions at all higher bifurcations are *always* unstable, at least in a finite neighborhood of the bifurcation from the trivial solution. In the linear regime these solutions have certain symmetry properties. They are either symmetric or antisymmetric about the equator and they can also be symmetric about the rotation axis. Krause and Meinel pointed out that the type of symmetry of the magnetic field realized in a dynamo model is determined by its stability properties. An unstable field configuration will evolve to another within a relatively short time. These investigations were based on a one-dimensional model. Brandenburg *et al.* (1989, hereinafter referred to as Paper I) considered the stability properties of axisymmetric (two-dimensional) fields in more complex mean-field dynamo models, such as α^2-dynamos in a sphere, where the dynamical interaction with the mean field flow is included simultaneously. Also $\alpha\omega$-dynamos have been found in which, for certain dynamo numbers, only (unsteady) solutions with mixed parities are possible. The models discussed in Paper I are just some few examples of an

obviously rich variety of different possibilities. The goal of the present paper is, therefore, to extend the parameter range of these investigations, and to attempt to gain new insight into the phenomena involved.

2. MODELS WITH BACK-REACTION ON THE MEAN FLOW

Proctor (1977) studied α^2-dynamos of dipolar parity which included the dynamical interaction with a self-consistently calculated mean flow in the presence of rotation. His main interest was to investigate the possibilities of a magnetostrophic state, where the Lorentz force is balanced only by the Coriolis force and other, gradient, terms. He did this by integrating the time-dependent, incompressible MHD-equations in a sphere assuming axisymmetry. We write these equations here in the following dimensionless form:

$$\frac{\mathrm{D}\mathbf{u}}{\mathrm{D}t} = -\operatorname{grad}\mathscr{P} - Ta^{1/2}\hat{\mathbf{z}}\times\mathbf{u} - \mathbf{B}\times\operatorname{curl}\mathbf{B} + P_m\nabla^2\mathbf{u}. \tag{1}$$

$$\frac{\partial\mathbf{B}}{\partial t} = \operatorname{curl}(\mathbf{u}\times\mathbf{B} + \alpha\mathbf{B} - \operatorname{curl}\mathbf{B}), \tag{2}$$

$$\operatorname{div}\mathbf{u} = \operatorname{div}\mathbf{B} = 0, \tag{3}$$

where $Ta = (2\Omega R^2/\nu)^2$ is the Taylor number and $P_m = \nu/\eta$ the magnetic Prandtl number (ν and η are kinematic viscosity and magnetic diffusivity, and R is the radius of the conducting sphere). $\mathscr{P}$ is a reduced pressure (which can contain also gravitational and centrifugal potentials), and the other quantities have their usual meaning. The time unit is the *magnetic* diffusive time, R^2/η, as is usual in dynamo theory. Taking the radius R as the unit of length, the velocity and the magnetic field are measured in units of η/R and $\sqrt{(\mu\rho)}\eta/R$, respectively. Here ρ is the constant density and μ the magnetic permeability. Both kinetic and magnetic energies are measured in units of $\rho(\eta/R)^2$. Outside the sphere we assume a vacuum, which implies $\operatorname{curl}\mathbf{B} = 0$. This leads to a boundary condition for $\mathbf{B}$ on $r = R$, which is handled using a method described by Jepps (1975). The boundary is assumed to be stress free, so angular momentum is conserved. Since we restrict ourselves to axisymmetric fields it is possible to solve this problem in terms of stream functions for $\mathbf{u}$ and $\mathbf{B}$ together with their azimuthal components. We use a numerical method similar to that of Proctor (1977).

Proctor noted the occurrence of persistent oscillations for high Taylor numbers, which he interpreted as an indication of a lack of stability of the magnetostrophic state. On approaching this magnetostrophic limit, these oscillations require not only a very high temporal resolution, but also long computational times, until a final solution is reached. The question arises whether this instability might allow the system to evolve to a new state of another symmetry type (or perhaps even to a state of mixed parity).

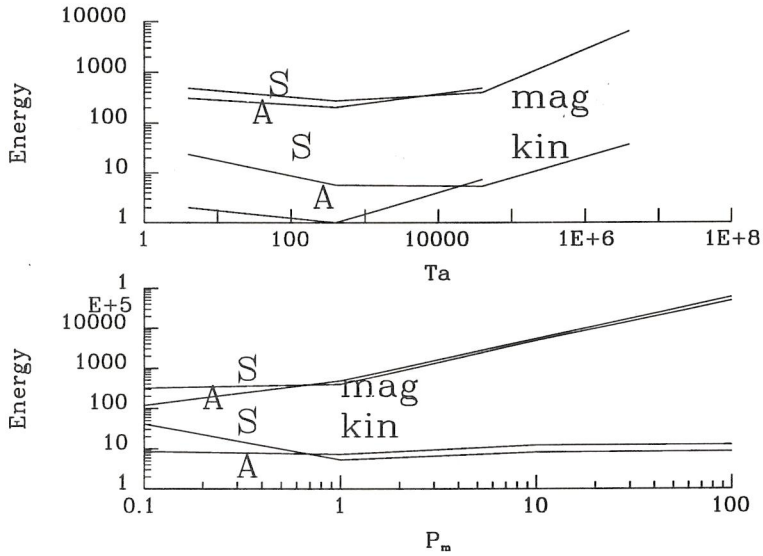

Figure 1 The total magnetic energy and the kinetic energy of the meridional circulation versus Taylor number for $P_m = 1$ (upper panel) and magnetic Prandtl number for $Ta = 4 \times 10^4$ (lower panel). α is constant in time and the dynamo number $C_\alpha = 10$.

Our code to solve equations (1)–(3) uses a difference scheme defined on the range $0 \leqq \theta \leqq \pi$ (θ the polar angle; unlike that of Proctor which was restricted to the range $0 \leqq \theta \leqq \pi/2$). Thus the parity type of our solutions is not pre-selected by boundary conditions on $\theta = \pi/2$ and solutions of either or mixed parities are always accessible (see Paper I for details). We have computed numerically several solutions with different values of Ta and P_m and $\alpha = C_\alpha \cos\theta$, where C_α is a dynamo number. For the models described in this section we have taken always $C_\alpha = 10$. In Figure 1 we have plotted the dependence of the total magnetic energy, E_{mag}, and the kinetic energy of the meridional circulation, E_{kin}, on Taylor number (upper panel) and on magnetic Prandtl number (lower panel). We denote by E_{mag} the energy of the mean magnetic field inside the sphere, *i.e.* $E_{\text{mag}} = \frac{1}{2}\int dV \mathbf{B}^2$. Similarly, E_{kin} refers to the kinetic energy of the mean meridional motion, *i.e.* $E_{\text{kin}} = \frac{1}{2}\int dV \mathbf{u}_{\text{mer}}^2$. The solutions can be symmetric or antisymmetric with respect to the equatorial plane. We call the symmetric solutions "S-type", "even" or "quadrupolar", and the antisymmetric solutions "A-type", "odd" or "dipolar". Both magnetic and kinetic energy at first decrease with increasing Taylor number, but for $Ta > 500$ they increase with Ta. The magnetic energies of the A- and S-type solution become asymptotically equal for large Ta and also for large P_m. The same is the case for the kinetic energies of both solutions.

2.1 Stability of the solutions

Having obtained a solution, we investigated its stability by perturbing it with another solution of opposite symmetry type. We then monitored the quantity:

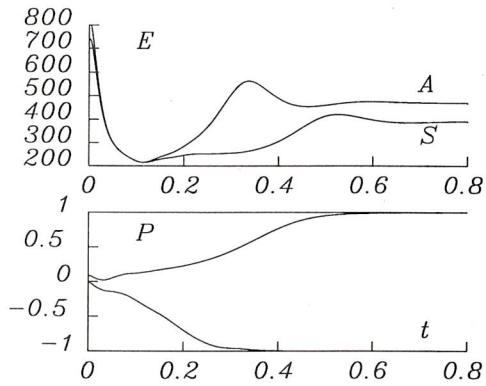

Figure 2 The evolution of E and P for a dynamo model with $Ta=4\times10^4$ and $P_m=1$. The type of symmetry finally established in the model depends on the relative contribution of $E^{(S)}$ and $E^{(A)}$ in the initial state.

$$P=\frac{E^{(S)}-E^{(A)}}{E^{(S)}+E^{(A)}}, \tag{4}$$

where $E^{(S)}$ and $E^{(A)}$ are the energies of the symmetric and antisymmetric part of the magnetic field. The quantity P was used quite frequently in Paper I. For pure symmetric solutions we have $P=1$, while for pure antisymmetric solutions $P=-1$.

In Figure 2 we have plotted the evolution of P for a dynamo model with $Ta=4\times10^4$ and $P_m=1$. This shows that the type of symmetry finally established in the model depends on the relative contribution of $E^{(S)}$ and $E^{(A)}$ to the initial condition. This is consistent with similar results in Paper I, where only the case $Ta=4$ was considered. Also for smaller $P_m=0.1$ we find that pure solutions are stable, but when starting with a "fully mixed" solution with $P\approx0$ we were not able to follow the evolution of the model. This was presumably because of numerical instability, which could not even be avoided with extremely short timestep (*e.g.* $\times200$ shorter). Similar numerical problems arise for larger Taylor numbers so that the stability of these solutions is still uncertain.

2.2 Stabilisation of solutions with pure parities

We shall now describe some properties of the solutions and their stability behavior. Particular attention will be paid to the variation of the mean flow as the parity of the solution changes. In Paper I it was argued that the spatial dependence of the feedback may be responsible for stabilizing either parity, at least when C_α exceeds a certain value. The feedback limiting the magnetic field strength is, in the present case, mainly the differential rotation produced by the Lorentz force. This differential rotation tends to quench the toroidal magnetic field. However, the field geometry, displayed in Figure 3, is more complicated than in the case, where the feedback comes only through an α-effect, which depends on $\mathbf{B}$ (see Figure 7 of Paper I). Two toroidal field belts develop in the southern

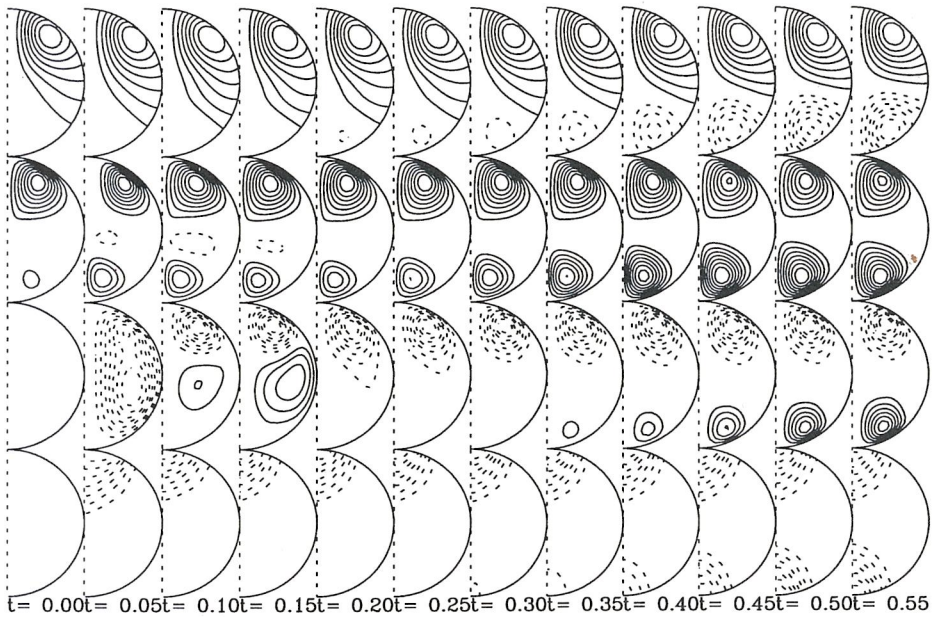

Figure 3 Poloidal field lines (first line), lines of constant toroidal field strength (second line), streamlines of meridional circulation (third line) and contours of constant angular velocity (last line) for the dynamo model in Figure 2 starting with $P=0.1$. In this case the final field geometry is even. The dashed lines denote a negative value.

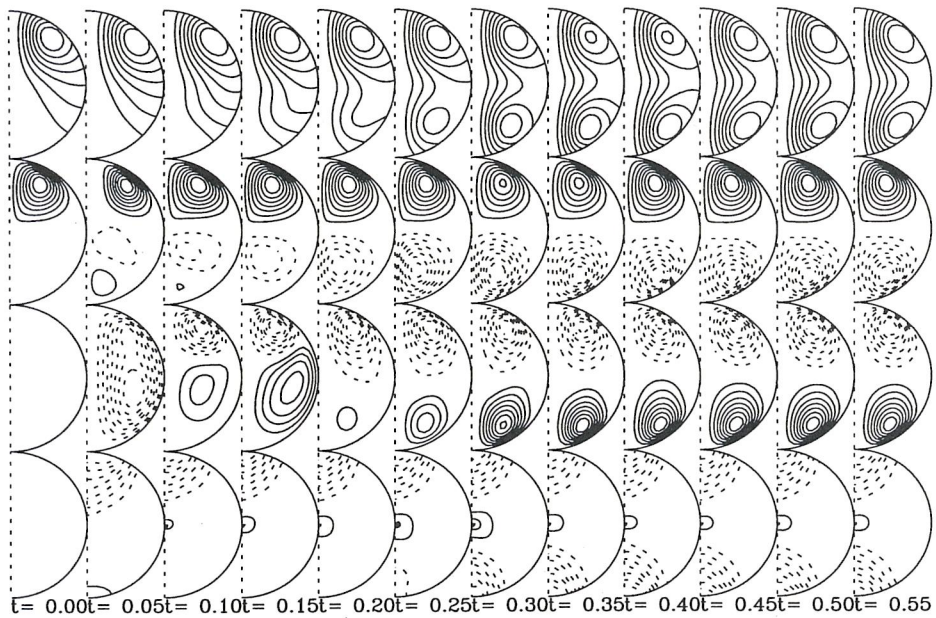

Figure 4 Same as Figure 3, but starting with $P=0.0$. In this case the final field geometry is odd. Note the oscillatory behaviour of the meridional circulation pattern on a time scale somewhat longer than the Alfvén time (≈ 0.05).

hemisphere ($t=0.1$), while there is only one in the northern hemisphere. The meridional motions behave quite violently and are oscillatory in the beginning, but their rôle in stabilizing field configurations may be minor compared to the toroidal motion. Figure 4 is similar, but starting with slightly smaller P. In this case the final field geometry is odd, and not even as in the previous case.

3. $\alpha\omega$-DYNAMOS

Section 6.4 of Paper I considered an $\alpha\omega$-dynamo with constant prescribed differential rotation, $\partial\Omega/\partial r \equiv C_\omega = -10^4$. The feedback of the magnetic field on the mean motions was, however, neglected, *i.e.* only the induction equation (2) was solved, although α was allowed to depend on the mean magnetic field via:

$$\alpha = \alpha(r,\theta) = \frac{C_\alpha \cos\theta}{1+\mathbf{B}(r,\theta,t)^2}. \tag{5}$$

Note that we have omitted any scaling factor in front of $\mathbf{B}^2$ in (5), because it would only renormalize the total magnetic energy of the solution. Therefore the energy is now of order unity, in contrast to the values of the energies in the previous section.

We should mention here that it is not clear at present what type of nonlinearity is the most important one limiting the magnetic field strength in the Sun and in stars, and on the other hand in the Earth and in planets. Spiegel and Weiss (1980) and Noyes *et al.* (1984) have argued that buoyancy is the most important mechanism in stars. Dynamos limited by magnetic buoyancy, and their stability properties, will be the subject of a further paper (Moss *et al.*, 1989). Here we shall restrict ourselves to the simple α-quenching mechanism. Results obtained in Paper I will be discussed and examined in more detail.

3.1 Solutions with mixed parity

While studying the stability of oscillatory, nonlinear $\alpha\omega$-dynamos it was found that in a certain range of C_α neither *purely* symmetric, nor *purely* antisymmetric solutions were stable. Perturbing a pure solution leads to persistent quasi-periodic oscillations with variable P. In Paper I an example of such a solution with $C_\alpha=0.9$ was given. On a long term period of approximately 10 times the basic magnetic cycle period the quantity P varied between positive and negative values, but never reached exactly plus or minus unity. In Figure 5 we have plotted the variation of the magnetic energy and the quantity P for the case $C_\alpha=0.85$. In contrast to the case with $C_\alpha=0.9$ the solution has for about 50% of the time the value $-1<P<-0.9$, *i.e.* it is most of the time nearly of dipolar type. However, bursts appear regularly bringing the system for brief intervals to nearly $P=+0.8$. Figure 5 shows also that at the same time the energy drops to very small values.

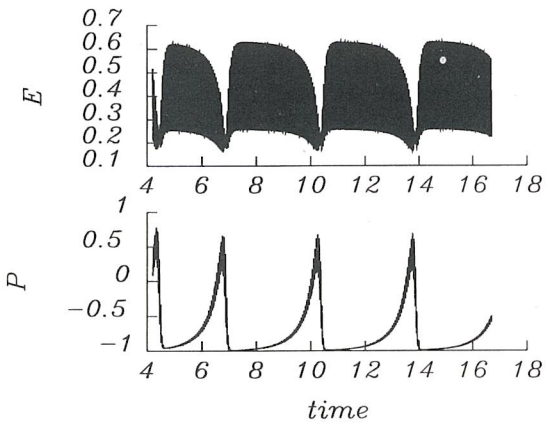

Figure 5 The variation of the magnetic energy (upper panel) and the quantity P for the case $C_\alpha = 0.85$. The "grand minima" in the energy correspond to strong deviations from the mainly dipolar symmetry type. The energy is here much smaller than in previous cases (Figures 1 and 2), because of the different nonlinear feedback, which is given here by Equation (5).

Somewhat speculatively one might ask whether during the solar Maunder minimum there were also clear deviations from the odd magnetic field parity. One might also note that such a phenomenon would appear on a single hemisphere as a sudden "field reversal", of the sort that is familiar from terrestrial magnetic records.

In Paper I we commented that for the case $C_\alpha = 0.9$ the long period was approximately equal to the beat frequency of the two pure solutions. Further calculations, presented in Table 1, suggested that this is not a general property of the solution.

3.2 Poincaré maps

In the language of nonlinear dynamics a periodic oscillatory solution, such as the magnetic cycle of a pure solution, can be described as a limit cycle in some phase space. The fact that the mixed solutions from the previous section show two distinct periods suggests that the trajectories of the solution lie on a torus in some phase space. In order to confirm this we projected the trajectories of the solutions onto a suitable hyperplane in the phase space. The dependent variables are in our case the ϕ-component of the magnetic vector potential A and the ϕ-component of the magnetic field B. For the numerical computations we used 40×81 gridpoints (in r and θ-directions respectively) so that the dimension of our phase space is $2 \times 40 \times 81$. Figure 6 gives the trajectory of the solution projected on to the plane (a_1, b_1), where $a_1 = A(r = 3R/4,\ \theta = \pi/4)$ and $b_1 = B(r = 3R/4,\ \theta = \pi/4)$, and the corresponding Poincaré maps, showing the intersections with the hyperplane $B(r = 3R/4,\ \theta = 3\pi/4) = 0$ for $C_\alpha = 0.75$ and 0.90. A different situation is met for $C_\alpha = 0.8$. In this instance the trajectory and the Poincaré map, shown in Figure 7, result from a small disturbance of a S-type solution. The solution approaches first

Table 1 Summary of some solutions of the $\alpha\omega$-dynamo for different C_α. The table is not complete, but contains only solutions found so far. In the first column is indicated their stability (s for stable, u for unstable). The third column, denoted with E, gives the minimum and maximum values of the total magnetic energy. The next column contains the value of P. In the case of mixed solutions the range covered by P is indicated. Ω_m is the magnetic cycle frequency, and Ω_m^* the frequency of the long-term oscillation. The latter coincides with the beat frequency (given in the last row) only for $C_\alpha = 0.9$

	C_α	E	P	Ω_m	Ω_m^*	
s	0.78	0.20...0.50	−1	59.1	0	
u	0.79	0.08...0.20	+1	66.4	0	
s		0.14...0.35	−0.41...−0.13	59.0	0	7.4
s		0.20...0.62	−1	61.3	0	
u	0.80	0.09...0.23	+1	67.6	0	
s		0.13...0.37	−0.46...+0.14	61.1	4.07	8.3
s		0.21...0.52	−0.91...−0.90	59.4	0	
s		0.21...0.54	−1	59.3	0	
u	0.81	0.12...0.30	+1	66.6	0	
s		0.16...0.50	−0.73...+0.40	59.4	0	
u		0.24...0.60	−1	59.3	0	
s	0.82	0.14...0.50	−0.78...+0.53	61.0	3.55	
u	0.83	0.16...0.39	+1	66.0	0	
s		0.15...0.56	−0.89...+0.54	62.8	3.06	
s		0.23...0.57	−0.88...−0.86	60.1	0	
u		0.16...0.64	−1	59.5	0	
s	0.85	0.16...0.63	−0.99...+0.67	60.5	1.80	
u	0.90	0.22...0.52	+1	68.3	0	
s		0.21...0.69	−0.79...+0.83	66.1	6.96	6.7
u		0.30...0.72	−1	61.6	0	
s	0.92		−0.61...+0.89	61.9	9.42	
s	0.94	0.25...0.74	−0.27...+0.92	67.6	12.4	
s	0.96	0.29...0.76	−0.10...+0.94	68.4	13.7	
s	1.00	0.34...0.81	+1	69.8	0	4.4
u		0.38...0.87	−1	65.4	0	
s	1.20	0.34...0.81	+1	71.4	0	0.0
u		0.38...0.87	−1	71.4	0	
s	1.50	0.34...0.81	+1	76.6	0	−1.9
u		0.38...0.87	−1	78.5	0	

a torus (right panel). This torus is obviously unstable, since after several revolutions a limit cycle is reached. The solution is, however, of mixed parity. This is shown in Figure 8. For some slightly different initial conditions, we find for the same dynamo number also a pure A-type oscillatory solution, which is shown in Figure 9. The limit cycle of this solution (Figure 10) lies well outside the region which is covered by the mixed solution (compare with Figure 8).

3.3 The transition from A- to S-type limit cycles

In this section we shall examine in more detail the solutions in the parameter

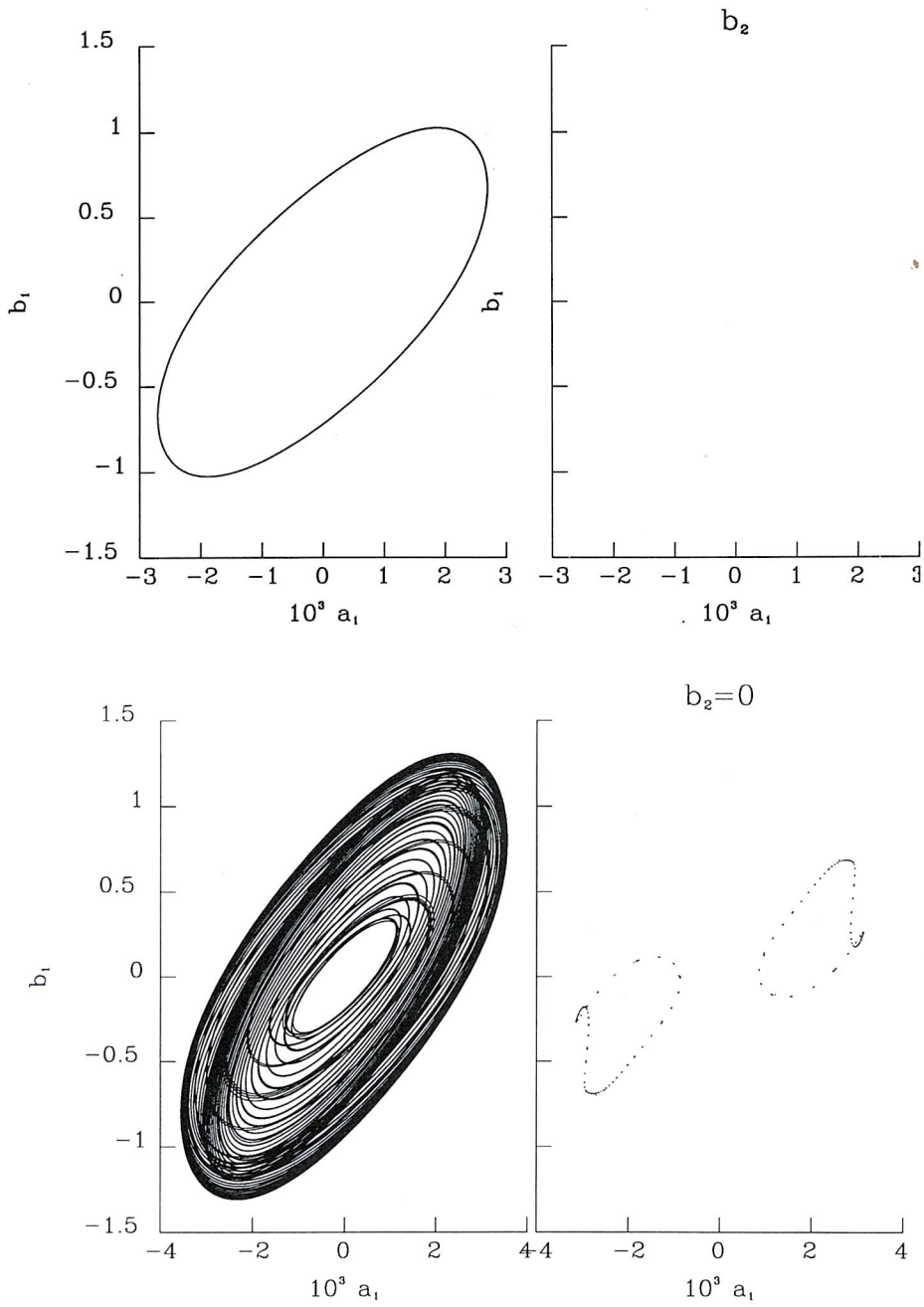

Figure 6 The trajectory of the solution in the plane $A(r=3R/4,\ \theta=\pi/4)$ and $B(r=3R/4,\ \theta=\pi/4)$. For $C_\alpha=0.75$ (upper left panel) the trajectory of the solution is a stable limit cycle. The corresponding Poincaré map (upper right panel) shows then only two points. For $C_\alpha=0.9$ (lower left panel) the trajectory of the solution looks now more confusing, but the corresponding Poincaré map (lower right panel) shows two rings, which indicate the boundary of a stable torus.

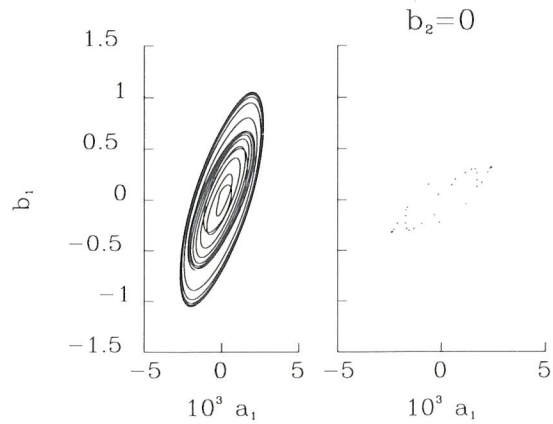

Figure 7 The trajectory and the Poincaré map for $C_\alpha=0.8$. The solution first approaches a torus (right panel). This torus is obviously unstable, since after several revolutions a limit cycle is reached, which is placed in the lower, left corner, as well as at the upper right edge.

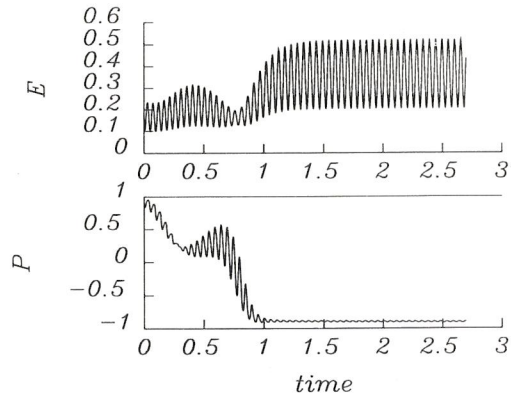

Figure 8 The variation of E and P for the solution shown in Figure 7. The final state is of mixed parity. This is an example of a mixed parity solution, which does not lie on a torus, but is a limit cycle.

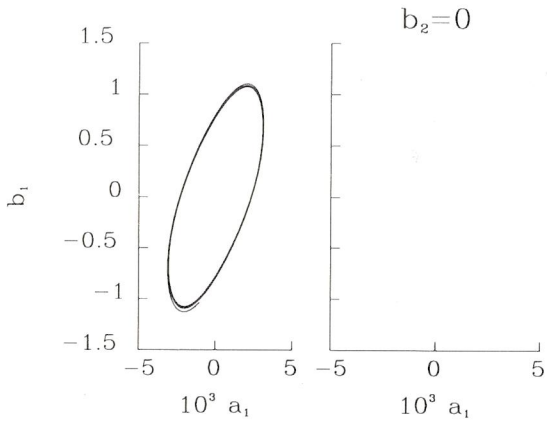

Figure 9 The same as Figure 7, but starting with another mixed solution, obtained for $C_\alpha=0.9$. Note that the Poincaré map consists only of two dots, which are located *outside* the region covered by the trajectory of the solution of Figure 7.

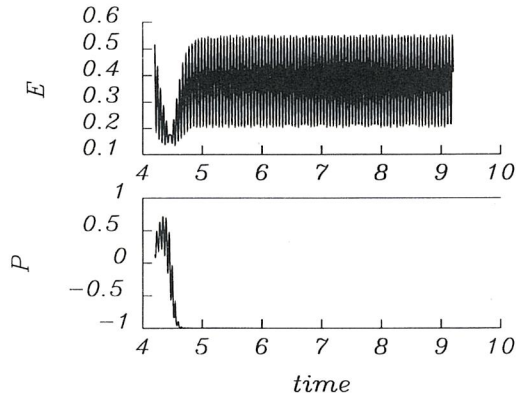

Figure 10 The variation of E and P for the solution shown in Figure 9. The final state is *not* of mixed parity, as in Figures 7 and 8.

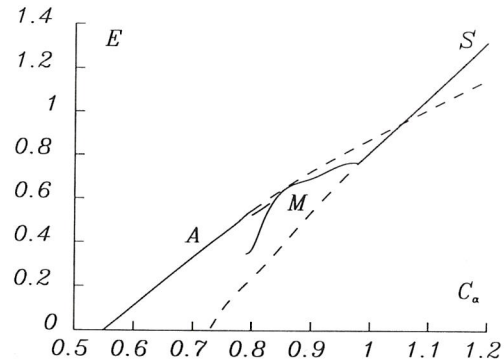

Figure 11 The maximum energies of the magnetic field versus dynamo number C_α. The solid line refers to stable solutions, whereas dotted lines indicate unstable solutions. The mixed mode branch, denoted by M, is a torus solution. For $0.80 \leqq C_\alpha \leqq 0.83$ there is another mixed mode branch, which is, however, a limit cycle solution. When $C_\alpha \approx 0.79$ the branch of torus solutions has also changed into limit cycle solutions. For even smaller C_α we have not been able to follow this branch any further.

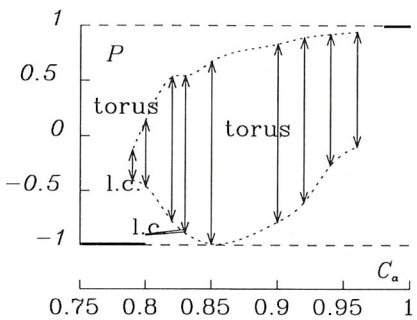

Figure 12 The solutions of the $\alpha\omega$-dynamo displayed in a $P-C_\alpha$-diagram. The range of P covered by stable torus solutions is indicated by arrows. The left-most arrow, however, belongs not to a torus, but to a limit cycle (l.c.). There are also "mixed-parity" limit cycle solutions for $0.80 \leqq C_\alpha \leqq 0.83$ (two lines at $P \approx -0.9$). The dashed and heavy lines for $P \pm 1$ are respectively unstable and stable solutions with pure parity.

range (C_α), where mixed solutions are possible. For $C_\alpha = 0.75$ only the A-type solution was found to be stable. The S-type solution, which already exists (positive growth rate), is, however, unstable. We then gradually increased C_α and always checked the stability of the solutions of pure symmetry type. For $C_\alpha \geqq 0.98$ we found the S-type solution to be stable. Mixed parity solutions, described in the previous section, could be followed in the range $0.79 \leqq C_\alpha \leqq 0.98$. The maximum energies of the magnetic field are plotted on a bifurcation diagram, shown in Figure 11. There is still another mixed-solution branch for $0.80 \leqq C_\alpha \leqq 0.83$, for which the attractor is presumably a limit cycle rather than a torus. However, we cannot exclude the possibility that this attractor is also a torus, for which the second period is too long to be found in our computations. This solution in the range $0.80 \leqq C_\alpha \leqq 0.83$ (limit cycle, denoted by l.c. in Figure 12) is obtained by starting the integration from a superposition of two solutions belonging to the same value of C_α, but with opposite symmetry type. In contrast, the torus-type solution is accessed in the same range of C_α by taking as initial condition a torus solution belonging to another (larger) value of C_α. We were not able to follow a mixed parity solution into the range $C_\alpha < 0.79$. The reason may be that such a solution is unstable in this range. It is a consequence of the method of stepping forward in time that we cannot find an unstable mixed-parity solution. It is therefore impossible to close the "loose ends" in the bifurcation diagram (Figure 11) and in Figure 12.

4. CONCLUSIONS

The calculations reported here develop two models for strictly axisymmetric nonlinear dynamos in spherical geometry that were first introduced in Paper I. Whilst these models do not yet show all the richness of bifurcations found in the very highly parameterized "toy" systems with $O(1\text{–}10)$ independent variables that have been extensively studied in the last few years (*e.g.* Jones *et al.*, 1985), they are one step nearer physical "reality" and the phenomena they reveal may possibly have more relevance to astrophysical systems.

The calculations of Section 2 for dynamically consistent models of α^2-type (with only small differential rotation, generated by the Lorentz force) demonstrated that the sensitivity of the parity of the final solution to the choice of initial conditions persists for a wide range of Taylor numbers, at least when the Prandtl number is unity. Our experiments approach, but probably do not quite attain, solar values of Ta, and may be still further from the terrestrial values.

In Section 3 we considered $\alpha\omega$-dynamos in which the nonlinearity is restricted to the α-quenching of (5). We have shown something of the richness of behaviour displayed in a certain range of C_α values—in particular the existence of a "window" where stable modes of either purely odd or purely even parity cannot be found and where, typically, the trajectory of the solution in its high-dimensional phase space is a torus. The potential richness of behavior of our system is apparent from the results presented.

The calculations are computationally time consuming and, unlike many of the

systems previously investigated (*e.g.* Jones *et al.*, 1985), it is not possible to do more than look at a few points in parameter space. Clearly we can make no claims about the full range of properties of our models, and it is very probable that more "interesting" parameter values exist. In particular we have not found any evidence for chaotic behaviour. Additional modelling of physical processes might be incorporated, introducing further nonlinearities (and parameters!). One obvious limitation of all our analyses is the restriction to strict axisymmetry. Our methods do not allow us to test the stability of our solutions to nonaxisymmetric perturbations. There is a suggestion from the work of Rädler and Wiedemann (1989) that some of our apparently stable solutions might be unstable to such perturbations—clearly this is an important question. Of course a nonlinear model that is not restricted to be axisymmetric offers many new possibilities for interesting behaviour including, for example, solutions which are mixtures, possibly unsteady, of axisymmetric and nonaxisymmetric modes!

References

Brandenburg, A., Krause, F., Meinel, R., Moss, D. and Tuominen, I., "The stability of nonlinear dynamos and the limited role of kinematic growth rates," *Astron. Astrophys.* **213,** 411–422 (1989).

Jepps, S. A., "Numerical models of hydromagnetic dynamos," *J. Fluid Mech.* **67,** 625–646 (1975).

Jones, C. A., Weiss, N. O. and Cattaneo, F., "Nonlinear dynamos: A generalization of the Lorentz equations," *Physica* **14D,** 161–174 (1985).

Kleeorin, N. I. and Ruzmaikin, A. A., "Mean-field dynamo with cubic non-linearity," *Astron. Nachr.* **305,** 265–275 (1984).

Krause, F. and Meinel, R., "Stability of simple nonlinear α^2-dynamos," *Geophys. & Astrophys. Fluid Dyn.* **43,** 95–117 (1988).

Moss, D., Tuominen, I. and Brandenburg, A., "Nonlinear dynamos with magnetic buoyancy in spherical geometry," *Astron. Astrophys.*, in press (1989).

Noyes, R. W., Weiss, N. O. and Vaughan, A. H., "The relation between stellar rotation rate and activity cycle periods," *Astrophys. J.* **287,** 769–773 (1984).

Proctor, M. R. E., "Numerical solutions of nonlinear α-effect dynamo equations," *J. Fluid Mech.* **80,** 769–784 (1977).

Rädler, K.-H. and Wiedemann, E., "Numerical experiments with a simple nonlinear mean-field dynamo model," *Geophys. & Astrophys. Fluid Dyn.* this issue (1989).

Spiegel, E. A. and Weiss, N. O., "Magnetic activity and variation in the solar luminosity," *Nature* **287,** 616–617 (1980).